09,07

Investigation of the $LiNO_3-KNO_3-LiClO_4$ salt system

© A.M. Amirov, M.A. Akhmedov, Z.Yu. Kubataev, M.M. Gafurov, K.Sh. Rabadanov, M.B. Ataev, M.V. Kadiev

Dagestan Federal Research Center of the Russian Academy of Sciences, Amirkhanov Institute of Physics, Analytical Center for Collective Use, Makhachkala, Russia

E-mail: aamirov@mail.ru

Received September 11, 2024
Revised September 24, 2024
Accepted September 24, 2024

The $LiNO_3-KNO_3$ nitrate eutectic was investigated at different additions of lithium perchlorate by methods of differential scanning calorimetry, X-ray diffraction and Raman spectroscopy, and data on electrical conductivity were obtained. It was found that the addition of lithium perchlorate to the nitrate eutectic leads to an increase in the specific ionic conductivity of the ternary salt system. It was found that with the increase of $LiClO_4$ addition the melting peak of $LiNO_3-KNO_3$ eutectic decreases and for the composition with the initial content of $0.5LiClO_4$ the phase transition of $LiNO_3-KNO_3$ eutectic is not registered, which is associated with the exchange reaction between potassium nitrate and lithium perchlorate with the formation of $KClO_4$ and $LiNO_3$. This conclusion is confirmed by X-ray diffraction of the system and Raman spectra, from which it follows that with increasing $LiClO_4$ addition the peak of full-symmetric valence vibration $\nu_1(KNO_3)$ decreases and the peak $\nu_1(KClO_4)$ is observed. When 0.5 mole fraction of $LiClO_4$ is added, the $\nu_1(KNO_3)$ peak completely disappears.

Keywords: alkali metal nitrates and perchlorates, ternary system, phase transitions, Raman scattering, X-ray phase analysis.

DOI: 10.61011/PSS.2024.11.60108.235

1. Introduction

Salt mixtures are widely used in various fields of science and technology. For example, for the production of many active metals by electrolysis, for the synthesis of various functional materials, etc. [1–6]. Eutectic mixtures of alkali metal nitrates are used in solar energy [7–9]. Nitrates and perchlorates are also used for the synthesis of solid composite electrolytes of „salt–oxide“ composition [10–14].

The main disadvantage of solid electrolytes is related to the relatively low ionic conductivity at room temperature. It is known that ionic conductivity in salt systems can be induced by both mobile cations and anions. Although the conductivity in energy storage systems is usually caused by the movement of metal cations, nevertheless, information about the mobility of the anionic subsystem may be extremely important for finding ways to increase the cationic conductivity of electrolytes. The strongest interparticle interactions in solid electrolytes are associated with Coulomb cation-anion interactions. These interactions lead to the formation of contact ion pairs that are unable to transfer charge, or inactive ion-associated complexes. In this regard, studies of ternary salt systems with various anions to a certain extent shed light on the dynamic features of anionic subsystems and contribute to the search for ways to increase cationic mobility in multicomponent solid electrolytes.

Despite the large number of publications on phase equilibria in different salt mixtures, systems containing different ions (different cations and anions) have been studied much less, and therefore studies of multicomponent salt systems are of considerable interest, both from a theoretical and practical point of view. However, there are a number of significant gaps in the understanding and description of the melting diagrams of mutual salt mixtures. The exchange reaction in the so-called mutual systems results in a number of significant features. Studies of multicomponent salt systems containing various anions are of interest in the light of the above.

The purpose of this paper is to study the effect of lithium perchlorate additives $LiClO_4$ on nitrate eutectic of $0.42LiNO_3-0.58KNO_3$ using differential scanning calorimetry, X-ray diffraction, vibrational spectroscopy, and electrical conductivity measurement.

2. Experimental methodology

$LiNO_3-KNO_3-LiClO_4$ salt systems of various compositions were prepared by using salts: lithium nitrate (c.p., „Ekros“), potassium nitrate (c.p., „Ekros“) and lithium perchlorate (extra pure, Sigma Aldrich). All work during the preparation of the studied samples was carried out in a dry glove box, in an inert atmosphere of high purity argon (99.9999 mass%). The initial salts $LiNO_3$, KNO_3 and $LiClO_4$ were dehydrated for 2 days by heating at 423 K and pumping in vacuum at residual pressure of 10^{-3} Pa, then they were placed in a glove vacuum box (Plas-Labs, USA).

Research methods. Differential scanning calorimetry (DSC) studies were performed using STA 449 F3 Jupiter thermal analyzer („NETZSCH“, Germany) from room

temperature to a preset temperature at a heating and cooling rate of 10 K/min in an argon atmosphere in platinum crucibles. Weight of samples 10 ± 1 mg. Temperature and sensitivity calibration was performed using standard substances (In, $RbNO_3$, KNO_3, $KClO_4$, Ag_2SO_4). Phase transition temperatures were determined based on the onset of the peak. The accuracy of temperature measurement is ± 1.5 K. Data processing and peak integration were carried out using embedded application programs of „NETZSCH".

X-ray diffraction patterns of the samples were acquired using XRD-7000 diffractometer (Shimadzu, Japan). The samples were a fine-grained powder, and no additional sample grinding was performed. The ready powder sample was placed in an Anton-PaarTTK-450 low temperature sample chamber stage, where it was first heated to a temperature of 120°C in a constant vacuum of a rotary vane pump and held for two hours for additional dehydration of the samples, and then measurements were conducted after cooling to room temperature. The X-ray diffraction patterns were measured using Bragg–Brentano focusing geometry; tube voltage 40 kV, current 30mA; X-ray wavelength $\lambda_{CuK\alpha} = 1.5406$ Å; nickel (Ni) filter on the primary beam; $\Theta-2\Theta$ scanning range — 15–100°, scanning step — 0.01°, exposure time per point — 20 s. The measurements were conducted at two temperatures: room temperature, $T = 25$°C (298 K), and $T = 120$°C (393 K).

The preliminary processing of the obtained diffraction patterns was performed using the Shimadzu software, it included: smoothing, background subtraction, $CuK_{\alpha 2}$ separation and subtraction, peak search, accounting for systematic errors in peak positions. The corresponding phases in the samples were searched using Search match program which searched in the ICDD (International Center for Diffraction Data)PDF-4+ (Powder Diffraction File) database, which includes more than 310 000 articles.

The specific ionic conductivity was investigated by electrochemical impedance spectroscopy (EIS) using a potentiostat-galvanostat P-45X with measurement module FRA-24M (Electrochemical Instruments, Russia) in the temperature range of 333–398 K in argon medium using a two-probe cell with graphite electrodes of 0.25 cm^2 area located at a distance of 0.4 cm from each other. Resistance values were obtained in the frequency range from 1 MHz to 1 Hz with the amplitude of the applied signal from 0.04 to 1 V.

From the parts of the linear relationship $1000/T - \lg\sigma$ obeying the Arrhenius equation (1), the angular coefficient (b) was determined by the least squares method, from which the activation energy (2) was determined:

$$\sigma = A\exp\left(-\frac{E_a}{RT}\right) \quad (1)$$

$$E_a = -b \cdot R \quad (2)$$

where σ is the specific electrical conductivity, S/sm; E_a is the activation energy, kJ/mol (or eV); T is the temperature, K; A is the coefficient characterizing the collision frequency of reacting molecules (energy barrier); R is the universal gas constant (8.31 J/(mol · K).

Raman spectra were recorded using Senterra confocal Raman microscope („Bruker" Germany). The Raman spectra were measured from room temperature to 350°C using thermal chamber that we designed for a confocal spectrometer [15] with laser excitation ($\lambda = 532$ nm and a power of 20 mW), the spectral measuring range of 50–1500 cm^{-1} with a resolution of 3–5 cm^{-1}, the integration time of each scan is 20 s. The samples were sealed in pyrex ampoules after removal of air and moisture from them using a vacuum pump at a temperature of 373 K.

The true contours of the bands were obtained by decomposition of spectra of the original complex contours of the spectrum bands into individual components, the shape of which was approximated by curves of the convolution form of the Gauss and Lorentz functions. The calculated curves and the initial spectrum were adjusted to minimize the absolute error using the Levenberg–Marquardt method. The error between the calculated and the real curve is 5–10%, depending on the signal-to-noise ratio of the original spectrum. All these processing procedures are implemented using the OPUS 6.0 software package.

3. Results and discussion

3.1. Conductivity

The specific ionic conductivity of the eutectic of $0.42LiNO_3-0.58KNO_3$ (hereinafter referred to as $(LiNO_3-KNO_3)_{eut.}$) and ternary salt systems $(1-x)(LiNO_3-KNO_3)_{eut.}-xLiClO_4$ was studied in the temperature range from 333 to 398 K, since softening of the sample with an uncontrolled change in its geometry was observed at temperatures above 398 K.

The data provided in Figure 1 for eutectic of $LiNO_3-KNO_3$ and ternary salt systems $(1-x)(LiNO_3-KNO_3)_{eut}-xLiClO_4$ are characterized by an abrupt increase of the specific ionic conductivity (SIC) at temperatures above ~ 393 K and two linear sections obeying the Arrhenius equation.

The presence of a structural phase transition and the formation of a metastable structure of potassium nitrate were studied in detail in Ref. [10–13]. The information about conductivity and structural features of a ternary salt system $(1-x)(LiNO_3-KNO_3)-xLiClO_4$ is not known. It can be assumed that the temperature dependences of conductivity observed in the experiment are related to changes in the crystal lattices of the components of the ternary system, competing processes of interaction between nitrate and perchlorate anions and cations with variations in temperature and concentration of $LiClO_4$.

Activation energy values of (E_a) are determined in Table 1 for linear sections obeying the Arrhenius equation (Figure 1).

The maximum value of the activation energy (1.28 eV) is observed at 333–373 K (Table 1) for

Table 1. Specific ionic conductivity and activation energy $(LiNO_3-KNO_3)_{eut.}$ and in the system $(1-x)(LiNO_3-KNO_3)_{eut}-xLiClO_4$

Composition	Temperature range, K					
	333–373			383–398		
	$\sigma \cdot 10^{-5}$, S/cm	E_a, eV	log A	$\sigma \cdot 10^{-3}$, S/cm	E_a, eV	log A
$0.42LiNO_3-0.58KNO_3$	0.052	0.82 ± 0.01	1.38	0.67	1.28 ± 0.04	2.57
$0.9(LiNO_3KNO_3)_{eut.}-0.1LiClO_4$	0.01	0.58 ± 0.02	0.12	2.63	0.37 ± 0.01	0.77
$0.8(LiNO_3-KNO_3)_{eut.}-0.2LiClO_4$	9.72	0.91 ± 0.03	2.01	7.70	1.09 ± 0.03	2.46
$0.7(LiNO_3-KNO_3)_{eut.}-0.3LiClO_4$	3.50	1.28 ± 0.03	2.83	2.19	0.53 ± 0.02	1.41

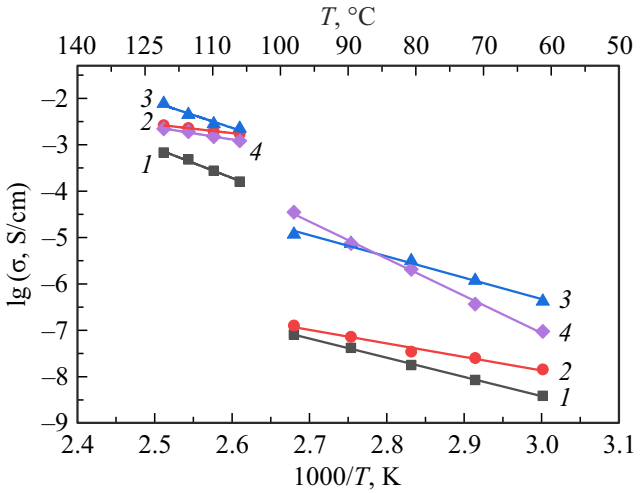

Figure 1. Temperature dependence of the specific ionic conductivity of eutectic of $LiNO_3-KNO_3$ (*1*) and ternary salt systems: $0.9(LiNO_3-KNO_3)_{eut.}-0.1LiClO_4$ (*2*), $0.8(LiNO_3-KNO_3)_{eut}-0.2LiClO_4$ (*3*) and $0.7(LiNO_3-KNO_3)_{eut}-0.3LiClO_4$ (*4*).

$0.7(LiNO_3-KNO_3)_{eut}-0.3LiClO_4$ system, whereas a low value of E_a (0.53 eV) is observed in the linear section at 383–398 K. Linear sections demonstrate relatively low values of E_a and constants logA at 333–373 K for $(LiNO_3-KNO_3)_{eut}$ and $0.9(LiNO_3-KNO_3)_{eut}-0.1LiClO_4$ in comparison with other studied systems. The activation energy for $0.9(LiNO_3-KNO_3)_{eut}-0.1LiClO_4$ system at 383–398 K is 3 times less than for eutectic of $LiNO_3-KNO_3$.

The value of the specific ion conductivity is maximum in $0.8(LiNO_3-KNO_3)_{eut}-0.2LiClO_4$ system at 398 K and is $7.70 \cdot 10^{-3}$ S/cm, which is an order of magnitude higher than the SIC for eutectic of $LiNO_3-KNO_3$. Linear sections are characterized by high values of the constant log A, tangent of the tilt angle, and the activation energy in the $0.8(LiNO_3-KNO_3)_{eut}-0.2LiClO_4$ system at 333–373 K and 383–398 K. This can be explained by the presence of phase transitions and related structural changes leading to an increase in the energy barrier. Moreover, the rate of transfer of charged particles in these electrolyte systems increase with the increase of the temperature.

3.2. Thermal analysis

It was found in Ref. [8,16,17] that eutectic in the binary salt system $LiNO_3-KNO_3$ is formed with the ratio of $LiNO_3$ and KNO_3 salts in molar fractions of 0.42 : 0.58 or values close to it. Previously, we studied composites based on $0.42LiNO_3-0.58KNO_3$ doped with nanoscale aluminum oxide, and found that heterogeneous doping affects the structure of nitrates and leads to an increase of the ionic conductivity [10,12].

Figure 2 shows the DSC heating curves of the ternary system $(1-x)(LiNO_3-KNO_3)-xLiClO_4$.

The melting peak of eutectic of $LiNO_3-KNO_3$ decreases with an increase of the content of lithium perchlorate as can be seen from Figure 2, which can be explained by a decrease of the proportion of nitrate eutectic of in the system. Obviously, an exchange reaction takes place between KNO_3 and $LiClO_4$ with the formation of potassium perchlorate and lithium nitrate:

$$KNO_3 + LiClO_4 = KClO_4 + LiNO_3$$

Thermodynamic analysis of the exchange reaction showed that the equilibrium is shifted towards the reaction products ($\Delta G < 0$). A phase transition appears on the DSC thermogram at ~ 478 K in parallel with the decrease of the

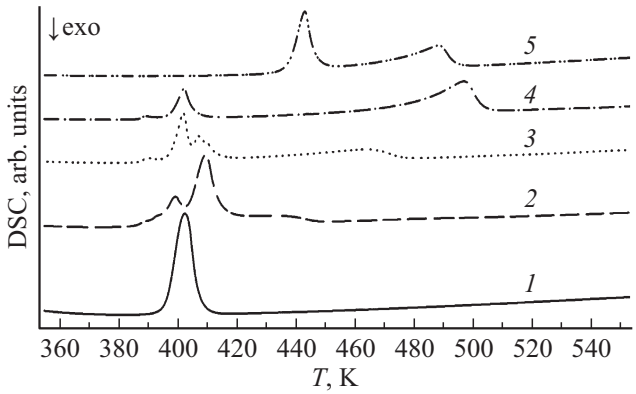

Figure 2. DSC heating curves of eutectic of $LiNO_3-KNO_3$ (*1*) and systems $(1-x)(LiNO_3-KNO_3)-xLiClO_4$, where $x = 0.1$ (*2*), 0.2 (*3*), 0.3 (*4*), 0.5 (*5*).

Table 2. Initial compositions $(1-x)(LiNO_3-KNO_3)-xLiClO_4$ and compositions possible as a result of the exchange reaction (both molar and mass fractions of components are indicated)

Initial composition	Salt compositions as a result exchange reactions (in mole fractions)				Mass fractions of components C, wt%			
	$LiNO_3$	KNO_3	$LiClO_4$	$KClO_4$	$LiNO_3$	KNO_3	$LiClO_4$	$KClO_4$
$(LiNO_3-KNO_3)_{eut}$	0.42	0.58	0	0	66.94	33.06	0	0
$0.9(LiNO_3-KNO_3)_{eut}-0.1LiClO_4$	0.478	0.422	0	0.1	36.8	47.7	0	15.5
$0.8(LiNO_3-KNO_3)_{eut}-0.2LiClO_4$	0.536	0.264	0	0.2	40.5	29.2	0	30.3
$0.7(LiNO_3-KNO_3)_{eut}-0.3LiClO_4$	0.594	0.106	0	0.3	43.9	11.5	0	44.6
$0.5(LiNO_3-KNO_3)_{eut}-0.5LiClO_4$	0.5	0	0.21	0.29	35.6	0	23	41.4

melting peak of the eutectic of $LiNO_3-KNO_3$. Table 2 shows the initial compositions and compositions possible as a result of the exchange reaction.

The phase transition of the eutectic of $LiNO_3-KNO_3$ is not recorded for a composition with an initial content of $0.5LiClO_4$ (Figure 2, curve *5*) which is obviously attributable to the absence of nitrate in the system potassium (Table 2). Thus, it can be assumed that all potassium nitrate was converted to potassium perchlorate for the composition with $x = 0.5$ as a result of the exchange reaction $KNO_3+LiClO_4 = KClO_4+LiNO_3$.

A phase transition is recorded at a temperature of 437 K on the curve *5* in addition to the absence of phase transitions of eutectic of $LiNO_3-KNO_3$ (Figure 2). This phase transition can be attributed to the melting of the mixture (eutectic) of $LiNO_3-LiClO_4$ [18].

The phase transition at ~ 478 K can be attributed to the melting of the mixture (eutectic) of $LiClO_4-KClO_4$ [19]. The registration of the phase transition on the curve *4* (Figure 2) at ~ 478 K can be explained by the incomplete transformation of $LiClO_4$ into $KClO_4$ by an exchange reaction and, consequently, the melting of eutectic of $LiClO_4-KClO_4$ is recorded on the thermogram.

3.3. Raman spectroscopy

The physical and chemical properties of the system are largely determined by the structure and behavior of the anions of the system. Raman scattering spectra were studied for a more complete interpretation of the effects of lithium perchlorate additives on the structure of eutectic of $LiKNO_3$. Molecular ions have internal degrees of freedom, which correspond to their own vibrations and which are reflected in the Raman spectra [10,12,20,21]. This can be used as an indicator that allows recording interparticle interactions and changes of the structure depending on temperature, concentration of various additives, etc.

It is known that the isolated molecular anion NO_3^- (symmetry D_{3h}) is characterized by the following internal oscillations: $\nu_1(A)$ is the full-symmetric stretching vibration ($\sim 1050\,cm^{-1}$), $\nu_2(E)$ is the out-of-plane deformation vibration ($\sim 820\,cm^{-1}$), $\nu_3(E)$ is the double degenerate asymmetric stretching vibration ($\sim 1300\,cm^{-1}$), $\nu_4(E)$ is the double degenerate deformation vibration ($\sim 720\,cm^{-1}$) [22].

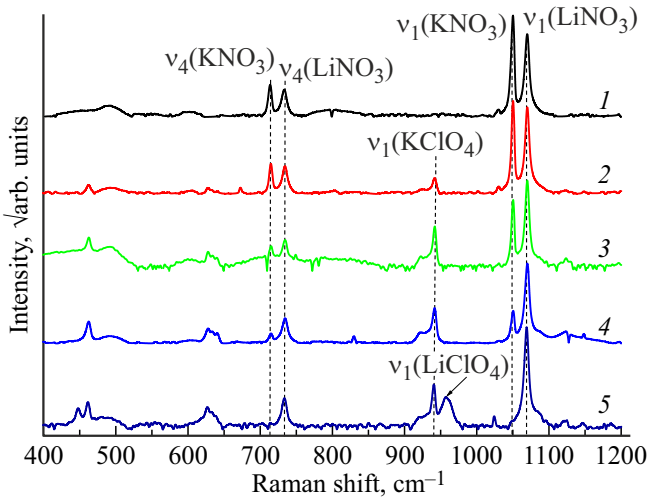

Figure 3. Raman spectra of $(1-x)(LiNO_3-KNO_3)-xLiClO_4$ system in the solid state at concentrations: 1) $x = 0$; 2) $x = 0.1$; 3) $x = 0.2$, 4) $x = 0.3$, 5) $x = 0.5$.

Figure 3 shows the Raman spectra of the studied systems in the solid and molten state in the oscillation range of $\nu_1(A_1^{\downarrow})$ of nitrate and perchlorate ions.

The salt system in the solid state provides spectra of the individual substances of this salt composition in accordance with their molar ratio. The intensity of the peak related to the fluctuation $\nu_1(A_1^{\downarrow})$ of potassium nitrate decreases ($\sim 1050\,cm^{-1}$) with the increase of the concentration of lithium perchlorate. A peak with a frequency of $941\,cm^{-1}$ is observed along with this, the intensity of which increases with the increase of $LiClO_4$ concentration. This peak belongs to the oscillation $\nu_1(A_1^{\downarrow})$ of $KClO_4$ [23]. The peaks of $\nu_1(KNO_3)$ and $\nu_4(KNO_3)$ completely disappear at concentrations of $x = 0.5$. These spectroscopic peculiarities confirms the conclusion made above about the occurrence of an exchange reaction in the system.

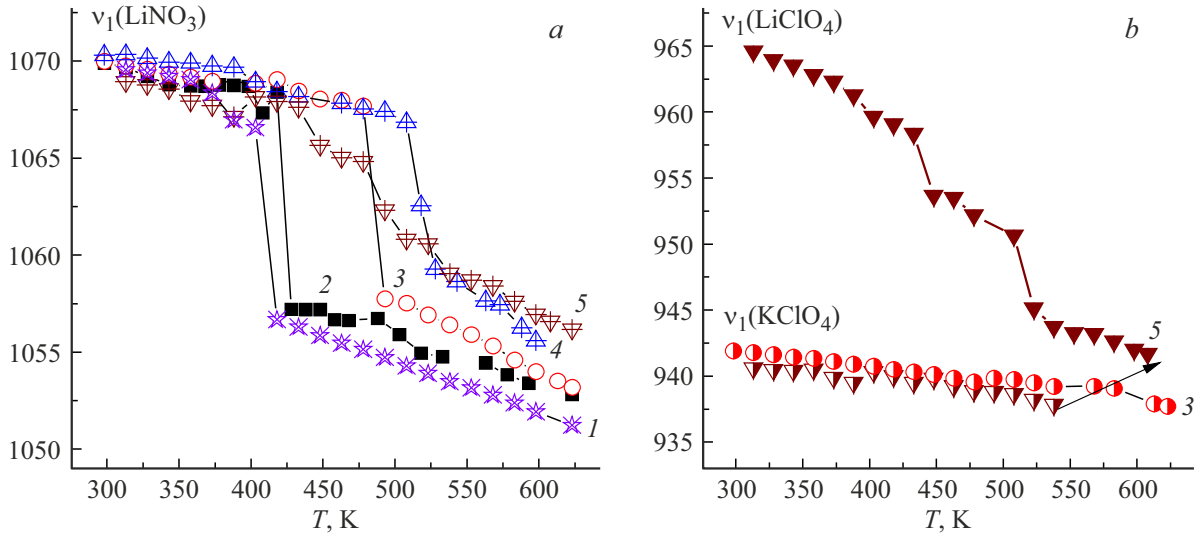

Figure 4. Temperature-phase dependence of frequencies ν_1 of a full-symmetric stretching vibration $\nu_1(A_1^{\downarrow})$ of the nitrate ion (a) and perchlorate ions (b) in Raman spectra with $LiClO_4$ concentrations: 1) $x = 0$; 2) $x = 0.1$; 3) $x = 0.2$, 4) $x = 0.3$, 5) $x = 0.5$.

Figure 4 shows the temperature and phase dependences of frequencies $\nu_1(A_1^{\downarrow})$ of nitrate (a) and perchlorate (b) ions. The values of frequency ν_1 ($LiNO_3$) do not depend on the perchlorate content in the solid state as can be seen from Figure 4. A concentration change of the frequency values of breathing mode ν_1 is observed for melts. The value ν_1 increased by $5\,cm^{-1}$ at the same temperature with the concentration of $x = 0.5$. Frequency shifts in the Raman spectra of salt melts indicate changes of the intermolecular interaction with changes of composition and temperature. An increase of the frequency $\nu_1(LiNO_3)$ and intensity values means an increase of the interaction of lithium ions with the nitrate ion of the mixture [24–27].

The oscillation frequency ν_1 of perchlorate ion in $KClO_4$ (Figure 4, b) almost does not change with a change of the concentration of lithium perchlorate, since the structural and vibrational characteristics of $KClO_4$ are attributable to stable and relatively isolated interactions within its crystal lattice. Lithium perchlorate at $x = 0.5$ forms eutectic of mixtures with lithium nitrate and potassium perchlorate with the increase of the temperature, at melting temperatures of which the frequency values $\nu_1(LiClO_4)$ abruptly change. It can be noted that the rate of frequency change $\nu_1(LiClO_4)$ is higher in the solid state than that of the other phases. This indicates a more disordered state of the lithium perchlorate subsystem.

3.4. X-ray powder diffraction

X-ray diffraction studies of samples of $0.8(LiNO_3-KNO_3)_{eut}-0.2LiClO_4$ and $0.7(LiNO_3-KNO_3)_{eut}-0.3LiClO_4$ were conducted (ratios are taken in mole fractions).

Since the structure of the binary eutectic of mixture of two salts $0.42LiNO_3-0.58KNO_3$, as well as its composites with nanoscale powder of γ-Al_2O_3 have already been studied by us previously [10,28,29], this time ternary systems based on this eutectic of with the addition of lithium perchlorate were studied.

As a result, the following phases were found:
– lithium nitrate, $LiNO_3$, (hexagonal (rhombohedral) lattice, R-3c, PDF-4+ chart 04-010-5519),
– potassium nitrate, KNO_3, (orthorhombic lattice, Pmna (phase II), PDF-4+ chart 04-008-9571),
– potassium perchlorate, $KClO_4$, (orthorhombic lattice, Pmna (β-phase), PDF-4+ chart 04-010-5417),
this confirms the above assumption about the exchange reaction between KNO_3 and $LiClO_4$ with the formation of potassium perchlorate and lithium nitrate.

After the phases included in the studied sample were determined, an estimated refinement of the crystal structures by the Rietveld method was carried out based on the initial diffraction patterns obtained. Highscore Plus v 3.0.5 software (PANalytical B.V., the Netherlands) was used for refinement. No other preliminary processing of diffraction patterns was performed, except for background determination. The lattice parameters of each of the phases were refined as a result of the Rietveld refinement and, in addition, the approximate content (C, wt%) of each of the phases was estimated. The accuracy of determination of the phase composition (%) by this method was $\pm 2-3\%$.

Table 3 below shows the refined values of the lattice parameters and the approximate phase content, the values of the divergence factors (R_p and R_{wp}) of the refined Rietveld model are additionally provided.

As can be seen from Table 3, the mass fractions of the components in the ternary systems obtained after a full-profile refinement, within the specified accuracy of determining the phase composition, coincide with the calculated values of the mass fractions of the components possible as a result of the exchange reaction (Table 2).

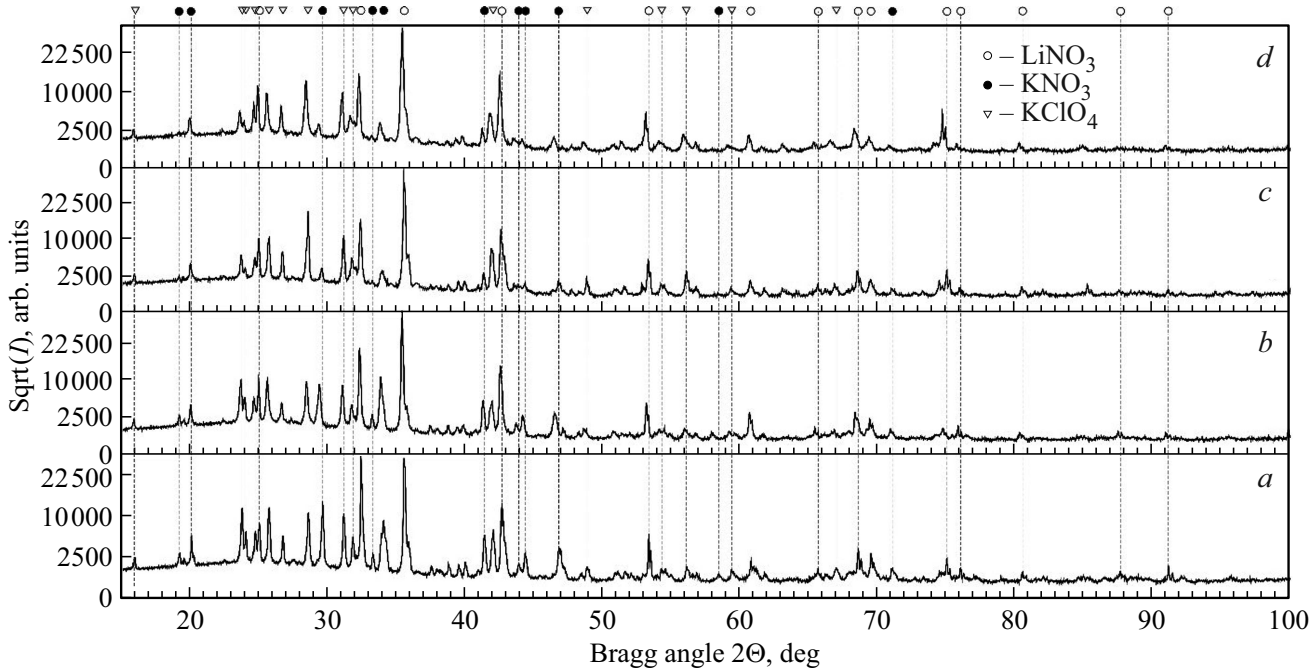

Figure 5. X-ray powder diffraction pattern of samples $(1-x)(LiNO_3-KNO_3)_{eut}-xLiClO_4$. *a* — $x = 0.2$, $T = 250^\circ$C (298 K); *b* — $x = 0.2$, $T = 120^\circ$C (393 K); *c* —$x = 0.3$, $T = 25^\circ$C (298 K); *d* — $x = 0.3$, $T = 120^\circ$C (393 K). Empty circles — lithium nitrate $LiNO_3$, R-3c; solid circles — potassium nitrate KNO_3, Pnma; triangles — potassium perchlorate $KClO_4$, Pnma.

Table 3. Refined values of lattice parameters and approximate content (C, wt%) of detected phases in samples of $(1-x)(LiNO_3-KNO_3)-xLiClO_4$, as well as the values of *R*-factors (divergence factors) of refinement

Composition	Lithium nitrate, $LiNO_3$, R-3c		Potassium nitrate, KNO_3, Pnma		Potassium perchlorate, $KClO_4$, Pnma		T, °C (K)	R_p	R_{wp}	GOF
x	Lattice parameters	C, wt%	Lattice parameters	C, wt%	Lattice parameters	C, wt%				
0.2	$a=b=4.6928(1)$ Å, $c=15.2271(2)$ Å, $\alpha=\beta=90^\circ$ $\gamma=120^\circ$	39 ± 1	$a=6.4368(2)$ Å, $b=5.4158(3)$ Å, $c=9.1639(6)$ Å, $\alpha=\beta=\gamma=90^\circ$	32 ± 1.5	$a=8.8625(4)$ Å, $b=5.6582(2)$ Å, $c=7.2569(3)$ Å, $\alpha=\beta=90^\circ$ $\gamma=120^\circ$	29 ± 1	25 (298)	10.8	15.2	29.7
0.2	$a=b=4.6977(2)$ Å, $c=15.2884(5)$ Å, $\alpha=\beta=90^\circ$ $\gamma=120^\circ$	41 ± 1	$a=6.4856(3)$ Å, $b=5.4224(3)$ Å, $c=9.1724(7)$ Å, $\alpha=\beta=\gamma=90^\circ$	29 ± 1	$a=8.9104(7)$ Å, $b=5.6717(4)$ Å, $c=7.2763(5)$ Å, $\alpha=\beta=90^\circ$ $\gamma=120^\circ$	30 ± 1	120 (393)	9.9	14.2	25.6
0.3	$a=b=4.6969(2)$ Å, $c=15.2212(4)$ Å, $\alpha=\beta=90^\circ$ $\gamma=120^\circ$	46 ± 1.5	$a=6.4421(7)$ Å, $b=5.4177(8)$ Å, $c=9.171(1)$ Å, $\alpha=\beta=\gamma=90^\circ$	11 ± 1	$a=8.8611(6)$ Å, $b=5.6626(3)$ Å, $c=7.2580(4)$ Å, $\alpha=\beta=90^\circ$ $\gamma=120^\circ$	43 ± 1	25 (298)	11.0	14.9	30.0
0.3	$a=b=4.7030(2)$ Å, $c=15.2754(5)$ Å, $\alpha=\beta=90^\circ$ $\gamma=120^\circ$	47 ± 2	$a=6.4896(8)$ Å, $b=5.4234(6)$ Å, $c=9.179(1)$ Å, $\alpha=\beta=\gamma=90^\circ$	10 ± 1	$a=8.9055(6)$ Å, $b=5.6776(4)$ Å, $c=7.2746(4)$ Å, $\alpha=\beta=90^\circ$ $\gamma=120^\circ$	43 ± 1	120 (393)	9.4	12.6	21.9

4. Conclusion

Thus, it can be concluded from the conducted studies that $LiNO_3-KNO_3$ binary eutectic and the ternary salt system $LiNO_3-KNO_3-LiClO_4$ are characterized by an abrupt increase of specific ionic conduction with two linear sections obeying the Arrhenius equation. The presence of an abrupt change of the conductivity is associated with phase transitions in the studied salt system. The addition of $0.1-0.3$ mole fraction of $LiClO_4$ to $LiNO_3-KNO_3$ eutectic leads to an increase of the specific ionic conductivity of the ternary salt system. In this case, potassium perchlorate, formed during the exchange reaction, plays the role of an active additive that promotes the growth of ionic mobility, in particular through competing mechanisms of anion-cation interactions, which are obviously characterized by electrolyte salt systems with different anions.

The melting peak of $LiNO_3-KNO_3$ the eutectic of decreases with an increase of the content of lithium perchlorate in the initial salt mixture. No phase transition of $LiNO_3-KNO_3$ eutectic is recorded for a composition with a starting content of $0.5LiClO_4$, which may be attributable to the exchange reaction $KNO_3 + LiClO_4 = KClO_4 + LiNO_3$. Interionic interactions in salt systems which change the local symmetry of NO_3^--ions, affect their transport and thermodynamic properties.

X-ray diffraction confirms the assumption that an exchange reaction takes place between KNO_3 and $LiClO_4$ with the formation of potassium perchlorate and lithium nitrate, while it was found that the mass fractions of all components with an accuracy of $2-3\%$ coincide with the calculated values of the components, possible as a result of the exchange reaction.

Funding

This study was supported by grant No. 24-23-00202 from the Russian Science Foundation, https://rscf.ru/prjcard_int?24-23-00202.
The study was conducted on the equipment of the Analytical Center for Collective Use of the Amirkhanov Institute of Physics of the Dagestan Federal Research Center of the Russian Academy of Sciences.

Conflict of interest

The authors declare that they have no conflict of interest.

References

[1] Yu.K. Delimarsky, L.P. Barchuk. Prikladnaya himiya ionnyh rasplavov. Nauk. Dumka, Kiev (1988). 192 p. (in Russian).
[2] M.V. Laptev, A.V. Isakov, O.V. Grishenkova, A.S. Vorob'ev, A.O. Khudorozhkova, L.A. Akashev, Yu.P. Zaikov. J. Electrochem. Soc. **167**, *4*, 042506 (2020). DOI: 10.1149/1945-7111/ab7aec
[3] A.A. Naberezhnov, O.A. Alekseeva, A.V. Kudryavtseva, D.Yu. Chernyshov, T.Yu. Vergentyev, A.V. Fokin. FTT **64**, *3*, 365 (2022). (in Russian). https://journals.ioffe.ru/articles/52098
[4] H. Liu, X. Zhang, S. He, D. He, Y. Shang, H. Yu. Materials Today **60**, 128 (2022). DOI: 10.1016/j.mattod.2022.09.005
[5] K. Jiang, Y. Shao, V. Smolenski, A. Novoselova, Q. Liu, M. Xu, Y. Yan, J. Yu, M. Zhang, J. Wang. J. Electroanal. Chem. **878**, 114691 (2020). https://doi.org/10.1016/j.jelechem.2020.114691
[6] M.M. Gafurov, K.Sh. Rabadanov, M.B. Ataev, A.M. Amirov, Z.Yu. Kubataev, M.G. Kakagasanov. FTT **57**, *10*, 2011 (2015). (in Russian). https://journals.ioffe.ru/articles/viewPDF/42270
[7] K. Coscia, S. Nelle, T. Elliott, S. Mohapatra, A. Oztekin, S. Neti. J. Sol. Energy Eng. **135**, *3*, 034506 (2013). https://doi.org/10.1115/1.4024069
[8] F. Roget, C. Favotto, J. Rogez. Solar Energy **95**, 155 (2013). https://doi.org/10.1016/j.solener.2013.06.008
[9] Z. Tong, L. Li, Y. Li, Q. Wang, X. Cheng. Materials **14**, *19*, 5737 (2021). DOI: 10.3390/ma14195737
[10] M.M. Gafurov, K.S. Rabadanov, M.B. Ataev, A.M. Amirov, M.A. Akhmedov, N.S. Shabanov, Z.Y. Kubataev, D.I. Rabadanova. Spectrochimica Acta **257**, 119765 (2021). https://doi.org/10.1016/j.saa.2021.119765
[11] A.M. Amirov, S.I. Suleymanov, M.M. Gafurov, M.B. Ataev, K.S. Rabadanov. J. Therm. Anal. Calorim. **147**, *17*, 9283 (2022). https://doi.org/10.1007/s10973-022-11256-0
[12] K.Sh. Rabadanov, M.M. Gafurov, Z.Yu. Kubataev, A.M. Amirov, M.A. Akhmedov, N.S. Shabanov, M.B. Ataev. Elektrokhimiya **55**, *6*, 750 (2019). (in Russian). 10.1134/S0424857019060173
[13] M.B. Ataev, M.M. Gafurov, R.M. Emirov, K.S. Rabadanov, A.M. Amirov. FTT **58**, *12*, 2336 (2016). (in Russian). https://journals.ioffe.ru/articles/43850
[14] A.S. Ulihin, N.F. Uvarov, Y.G. Mateyshina, L.I. Brezhneva, A.A. Matvienko. Solid State Ionics **177**, *26–32*, 2787 (2006). DOI: 10.1016/j.ssi.2006.03.018
[15] M.M. Gafurov, K.S. Rabadanov. Appl. Spectrosc. Rev. **58**, *7*, 489 (2023). DOI: 10.1080/05704928.2022.2048305
[16] C. Vallet. J. Chem. Thermodyn. **4**, *1*, 105 (1972). https://doi.org/10.1016/S0021-9614(72)80013-2
[17] M. Guizani, H. Zamali, M. Jemal. C.R. Acad. Sci. Paris **1**, *12*, 787 (1998). https://doi.org/10.1016/S1251-8069(99)80047-4
[18] V.I. Posypayko, E.A. Alekseeva, N.A. Vasina. Diagrammy plavkosti solevyh sistem: spravochnik. Ch. III. Dvojnye sistemy s obshchim kationom. Metallurgiya, M. (1979). 204 p. (in Russian).
[19] M.M. Markowitz, D.A. Boryta, R.F. Harri. J. Phys. Chem. **65**, *2*, 261 (1961). https://doi.org/10.1021/j100820a018
[20] E.V. Nikolaeva, I.D. Zakiryanova, A.L. Bovet, I.V. Korzun. J. Electrochem. Soc. **168**, *1*, 016502 (2021). DOI: 10.1149/1945-7111/abd64a
[21] A.R. Aliev, M.M. Gafurov, I.R. Akhmedov, M.G. Kakagasanov, Z.A. Aliev. FTT **60**, *6*, 1191 (2018). (in Russian). https://journals.ioffe.ru/articles/viewPDF/45999
[22] G. Herzberg. Kolebatel'nye i vrashchatel'nye spektry mnogoatomnyh molekul. IL, M. (1949). 647 p. (in Russian).
[23] H. Qu, Z. Ling, X. Qi, Y. Xin, C. Liu, H. Cao. Sensors **21**, *21*, 6973 (2021). DOI: 10.3390/s21216973
[24] A.G. Kalampounias, S.A. Kirillov, W. Steffen, S.N. Yannopoulos. J. Mol. Struct. **651–653**, 475 (2003). DOI: 10.1016/S0022-2860(03)00128-5

[25] A.G. Kalampounias. J. Phys. Chem. Sol. **73**, *2*, 148 (2012). DOI: 10.1016/j.jpcs.2011.11.014
[26] S.A. Kirillov. V kn.: Dinamicheskie svojstva molekul i kondensirovannyh sistem / Pod red. A.N. Lazareva. Nauka, L. (1988). P. 190. (in Russian).
[27] M.M. Gafurov, I.R. Akhmedov, A.R. Aliev. Zhurnal prikladnoy spektroskopii **52**, *3*, 429 (1990). (in Russian).
[28] A.M. Amirov, M.M. Gafurov, M.B. Ataev, K.Sh. Rabadanov. Appl. Solid State Chem. **3**, *12* (2018).
[29] M.M. Gafurov, K.Sh. Rabadanov, A.M. Amirov, M.B. Ataev, Z.Yu. Kubataev, M.G. Kakagasanov. ZHurnal strukturnoj khimii **60**, *3*, 422 (2019). (in Russian).

Translated by A.Akhtyamov